Title
A method for building a genome-connectome bipartite graph model.

Authors
Yu, Qingbao
Chen, Jiayu
Du, Yuhui
et al.

Publication Date
2019-05-01

DOI
10.1016/j.jneumeth.2019.03.011

Peer reviewed

HHS Public Access

Author manuscript

J Neurosci Methods. Author manuscript; available in PMC 2020 May 15.

Published in final edited form as:

J Neurosci Methods. 2019 May 15; 320: 64–71. doi:10.1016/j.jneumeth.2019.03.011.

A method for building a genome-connectome bipartite graph model

Qingbao Yu[1,#], **Jiayu Chen**[1,#,*], **Yuhui Du**[1,2], **Jing Sui**[1,3,4], **Eswar Damaraju**[1], **Jessica A. Turner**[5], **Theo G.M. van Erp**[6], **Fabio Macciardi**[6], **Aysenil Belger**[7], **Judith M. Ford**[8,9], **Sarah McEwen**[10], **Daniel H. Mathalon**[8,9], **Bryon A. Mueller**[11], **Adrian Preda**[6], **Jatin Vaidya**[12], **Godfrey D. Pearlson**[13,14,15], and **Vince D. Calhoun**[1,15,16,*]

[1.]The Mind Research Network, Albuquerque, NM, 87106, USA

[2.]School of Computer and Information Technology, Shanxi University, Taiyuan, 030006, China

[3.]Brainnetome Center and National Laboratory of Pattern Recognition, Institute of Automation, Chinese Academy of Science, Bijing, 100190, China

[4.]CAS Center for Excellence in Brain Science and Intelligence Technology, University of Chinese Academy of Sciences in Beijing, 100049, China

[5.]Department of Psychology, Georgia State University, GA, 30303, USA

[6.]Department of Psychiatry and Human Behavior, School of Medicine, University of California, Irvine, CA, 92697, USA

[7.]Department of Psychiatry, University of North Carolina, Chapel Hill, NC, 27514, USA

[8.]Department of Psychiatry, University of California San Francisco, CA, 94143, USA

[9.]San Francisco VA Medical Center, San Francisco, CA, 94121, USA

[10.]Department of Psychiatry and Biobehavioral Sciences, University of California Los Angeles, CA, 90095, USA

[11.]Department of Psychiatry, University of Minnesota, Minneapolis, MN, 55454, USA

[12.]Department of Psychiatry, University of Iowa, IA, 52242, USA

[13.]Olin Neuropsychiatry Research Center, Hartford, CT 06106, USA

[14.]Department of Neuroscience, Yale University, New Haven, CT 06520, USA

[15.]Department of Psychiatry, Yale University, New Haven, CT, 06520, USA

[16.]Department of Electrical and Computer Engineering, University of New Mexico, Albuquerque, NM, 87016, USA

[*]Corresponding author: Vince Calhoun (vcalhoun@unm.edu) and Jiayu Chen (jchen@mrn.org); The Mind Research Network, 1101 Yale Blvd NE, Albuquerque, NM87106, USA.

[#]These authors contributed equally to this work.

Abstract

It has been widely shown that genomic factors influence both risk for schizophrenia and variation in functional brain connectivity. Moreover, schizophrenia is characterized by disrupted brain connectivity. In this work, we proposed a genome-connectome bipartite graph model to perform imaging genomic analysis. Functional network connectivity (FNC) was estimated after decomposing resting state functional magnetic resonance imaging data from both healthy controls (HC) and patients with schizophrenia (SZ) into spatial brain components using group independent component analysis (G-ICA). Then 83 FNC connections showing a group difference (HC vs SZ) were selected as fMRI nodes, and eighty-one schizophrenia-related single nucleotide polymorphisms (SNPs) were selected as genetic nodes respectively in the bipartite graph. Edges connecting pairs of genetic and fMRI nodes were defined based on the SNP-FNC associations across subjects evaluated by a general linear model. Results show that some SNP nodes in the bipartite graph have a high degree implying they are influential in modulating brain connectivity and may be more strongly associated with the risk of schizophrenia than other SNPs. A bi-clustering analysis detected a cluster with 15 SNPs interacting with 38 FNC connections, most of which were within or between somato-motor and visual brain areas. This suggests that the activity of these brain regions may be related to common SNPs and provides insights into the pathology of schizophrenia. The findings suggest that the SNP-FNC bipartite graph approach is a novel model to investigate genetic influences on functional brain connectivity in mental illness.

Keywords

fMRI; FNC; SNPs; bipartite graph

1. Introduction:

Resting state functional magnetic resonance imaging (R-fMRI) is a popular non-invasive technique to investigate the characteristics of the human brain (Fox and Raichle, 2007; van den Heuvel and Hulshoff Pol, 2010). Functional connectivity (FC) analysis is a widely used and informative approach to analyze R-fMRI data (Biswal et al., 1995; Biswal, 2012; Friston, 2011; Friston et al., 1996). Functional network connectivity (FNC) analysis is a data driven method to compute the inter-network FC in R-fMRI data (Jafri et al., 2008). In this approach, group spatial independent component analysis (G-ICA) is firstly performed on R-fMRI data, and then brain components of interest are determined. Finally, an FNC matrix is constructed by computing the correlation values of each pair of ICA time courses of the brain components of interest (He et al., 2016). Using this method, disrupted brain connectivity between spatial brain components has been consistently shown in individuals with brain disorders such as schizophrenia (Arbabshirani and Calhoun, 2011; Arbabshirani et al., 2013; Arbabshirani et al., 2017; Du et al., 2018; Du et al., 2015). Graph measures of FNC in both healthy controls (HCs) and patients with schizophrenia (SZs) are also widely studied (Betzel and Bassett, 2016; van den Heuvel and Fornito, 2014; Yu et al., 2018; Yu et al., 2015; Yu et al., 2011a; Yu et al., 2013a; Yu et al., 2013b; Yu et al., 2011b). In addition, it has been demonstrated that, in some cases, data-driven ICA derived brain nodes outperform brain atlas based-ROI nodes for building a brain connectivity brain graph (Yu et al., 2017).

However, the genetic basis of brain FNC is largely unknown, though resting brain functional patterns are strongly heritable (Adhikari et al., 2018; Glahn et al., 2010), which motivated us to explore the associations of FNC with genetic variants.

It is well known that genetic factors influence both risk for schizophrenia and variation in functional brain connectivity. For example, heritability (the proportion of total variance in a trait due to genetic variation) has been estimated from family and twin studies at 81% for schizophrenia (Sullivan et al., 2003). Genome-wide association studies (GWAS) are increasingly used to characterize genetic risk profiles for schizophrenia (Potkin et al., 2009). In addition, numerous twin and family studies have provided strong evidence for heritability of diverse aspects of functional brain connectivity (Anokhin, 2014; Fu et al., 2015; Ge et al., 2017; Yang et al., 2016). Heritability of effective and functional connectivity in default mode network has been reported to be 0.54 (Xu et al., 2017), and 0.424 (Glahn et al., 2010) respectively. Heritability of graph measures in brain connectivity has also been investigated. A study with monozygotic and dizygotic twins has estimated the heritability of five graph metrics (clustering coefficient, modularity, rich-club coefficient, global efficiency, and small-worldness), and results show that the graph metrics are moderately influenced by genetic factors suggesting that these metrics may be potential endophenotypes for psychiatric diseases and suitable for genetic association studies (Sinclair et al., 2015). In a twin fMRI study involving young children, global efficiency of functional connectivity brain graphs have been found to be under genetic control (42%) implying that a set of genes is shaping the underlying architecture of functional brain communication during development (van den Heuvel et al., 2013). This also implies that neuroimaging parameters such as functional brain connectivity may be useful as endophenotypes.

The combination of neuroimaging and genetic analyses, or imaging genetics (Petrella et al., 2008), has been increasingly used in the past decade. By incorporating neuroimaging endophenotypes with the genetic data from healthy and/or disease subjects, the effects of genetic variations (such as SNPs) on brain structure and function can be assessed. Imaging genetics is a powerful way to link genetic factors to structural and functional variation in brain systems related to cognition and emotion (Meyer-Lindenberg and Weinberger, 2006). One strategy is to utilize endophenotypes derived from neuroimaging data to test the genetic association of a relatively well validated candidate gene of specific mental illness (Arslan, 2018). The other strategy is blind genome wide assessment, i.e. genome-wide association studies with imaging phenotypes serving as the trait. The common assumption of using intermediate imaging phenotype is that genetic variants present more direct effects at the level of the brain than complex behavior, and carriers of risk alleles may present brain abnormalities even if they show no clinical diagnostic characteristics. Imaging genetics therefore becomes a guide to the discovery of neural circuitry that translates genetic effects into behavior, and endophenotypes implicate endo-mechanisms (Meyer-Lindenberg and Weinberger, 2006).

In this work, we propose a genome-connectome multimodal bipartite graph model to perform imaging genetic analysis. A bipartite graph, also called a bigraph, is a set of graph nodes decomposed into two disjoint sets such that no two graph nodes within the same set are adjacent (Brualdi et al., 1980). Here we build a bipartite graph in which one group nodes

are schizophrenia-related SNPs and the other group nodes represent schizophrenia-related functional brain connectivity. Associations between nodes from these two sets are evaluated using a general linear model. This pilot study provides a novel framework by combining group ICA, bipartite graph analysis, and biclustering analysis to investigate possible genetic basis of the variations in functional brain connectivity and the risk of schizophrenia.

2. Materials and Methods:

2.1. Participants

A total of 97 HCs (30 female; 5 left handed; age: range 19 – 60; mean ± SD 37 ± 11) and 70 SZs (11 female; 1 left handed; age: range 18 – 60; mean ± SD 38 ± 11) from 7 research sites participated in this study. All participants provided written, informed consent in accordance with internal review boards of their corresponding institutions.

2.2. fMRI data acquisition

Brain imaging data were collected from 3T Siemens Tim Trio MRI Systems (6 of the 7 sites) and a 3T General Electric Discovery MR750 scanner (the other site). Resting state fMRI scans were acquired using a standard gradient-echo planar imaging paradigm: FOV of 220 × 220 mm (64 × 64 matrix), TR = 2 s, TE = 30 ms, flip angle = 70°, 32 sequential ascending axial slices of 4 mm thickness and 1 mm skip. A total of 162 brain volumes were acquired for each subject with eyes closed over 5 minutes and 24 seconds.

2.3. fMRI data preprocessing

FMRI data preprocessing was performed using a combination of toolboxes (AFNI: https://afni.nimh.nih.gov/; SPM: http://www.fil.ion.ucl.ac.uk/spm/; GIFT: http://mialab.mrn.org/software/gift) and custom Matlab code (https://www.mathworks.com/products/matlab.html). We performed rigid body motion correction using the INRIAlign (Freire et al., 2002) toolbox in SPM to correct for subject head motion followed by slice-timing correction to account for timing differences in slice acquisition. Then the fMRI data were de-spiked using AFNI's 3dDespike algorithm to mitigate the impact of outliers. The fMRI data were subsequently warped to a Montreal Neurological Institute (MNI) template and resampled to 3 × 3 × 3 mm isotropic voxels. Instead of Gaussian smoothing, we smoothed the data to 6 mm full width at half maximum (FWHM) using AFNI's BlurToFWHM algorithm which performs smoothing by a conservative finite difference approximation to the diffusion equation. This approach had been shown to reduce scanner specific variability in smoothness providing "smoothness equivalence" to data across sites (Friedman et al., 2006a; Friedman et al., 2006b). Each voxel time course was variance normalized prior to performing group ICA as this has shown to better decompose subcortical sources in addition to cortical networks (Allen et al., 2011; Damaraju et al., 2014).

2.4. Group ICA of fMRI

After preprocessing, fMRI of both controls and patients were analyzed using a spatial group ICA as implemented in GIFT software (Calhoun et al., 2001; Erhardt et al., 2011). Spatial ICA decomposes the subject data into linear mixtures of spatially independent components (ICs) that exhibit unique time course profiles. A subject-specific data reduction step was first

used to reduce 162-time-point data into 100 directions of maximal variability using principal component analysis (PCA). Then subject-reduced data were concatenated along the time dimension and a second PCA step reduced this grouped data matrix further into 100 components along directions of maximal group variability. One hundred ICs were obtained from the group PCA reduced matrix using the Infomax algorithm (Bell and Sejnowski, 1995). To ensure stability of estimation, we repeated the ICA algorithm 20 times in ICASSO (http://research.ics.aalto.fi/ica/icasso/), and the most central run was selected and further analyzed (Ma et al., 2011). Subject specific spatial maps (SMs) and time courses (TCs) were obtained using the spatiotemporal regression back reconstruction approach implemented in GIFT (Calhoun et al., 2001; Erhardt et al., 2011).

2.5. Post-ICA processing

Subject-specific SMs and TCs underwent post-processing as described in our earlier work (Allen et al., 2014). Briefly, we obtained one sample t-test maps for each SM across all subjects and thresholded these maps to obtain regions of peak activation clusters for that component. We also computed mean power spectra of the corresponding TCs. We identified a set of components as intrinsic connectivity networks (ICNs) if their peak activation clusters fell on gray matter and showed less overlap with known vascular, susceptibility, ventricular, and edge regions corresponding to head motion. We also ensured that the mean power spectra of the selected ICN time courses showed higher low frequency spectral power. This selection procedure resulted in 50 ICNs out of the 100 ICs obtained. The subject specific TCs corresponding to the 50 ICNs selected were detrended, despiked, and then band pass filtered (0.01 − 0.10 Hz) before the subsequent FNC analysis (Allen et al., 2014; Damaraju et al., 2014; Yu et al., 2015).

2.6. FNC analysis and the definition of connectome nodes

We constructed the FNC which is defined as pairwise correlations between ICN time courses, as a measure of connectivity among different ICNs during the scan duration for each individual. In this work, the FNC computed using the whole ICN time courses is referred to as stationary or static FNC (sFNC). The mean sFNC matrix across subjects was also computed in each group.

FMRI nodes in the gene-fMRI bipartite graph represent FNC connections in the sFNC matrix. Eighty-three fMRI nodes were selected by below criteria: 1. Correlation value of the group mean FNC connection of HCs is higher than 0.3268 ($r > 0.3268$). This criterion was determined based on the significant correlation between ICNs ($q < 0.05$, Bonferroni correction). 2. Group difference (HCs vs SZs) on the correlation value is significant ($q < 0.05$, false discovery rate [FDR] correction).

2.7. SNP data acquisition and processing

DNA of each subject was extracted from blood or saliva samples. Illumina Human Omni1-Quad, Illumina Human Omni5, and Illumina Infinium MEGA + Psych were used for genotyping. No significant difference was noted in genotyping call rates between blood and saliva samples. The data then went through quality control (QC), imputation and post-imputation QC as described in (Chen et al., 2018). In brief, a standard QC (Chen et al.,

2013) was firstly performed using PLINK (Purcell et al., 2007). Then imputation was conducted with SHAPEIT used for pre-phasing (Delaneau et al., 2011), IMPUTE2 for imputation (Marchini and Howie, 2010), and the 1000 Genomes data as the reference panel (Altshuler et al., 2012). Only markers with high imputation qualities (INFO score > 0.95) were retained. The imputed data were then aggregated and went through the post-imputation QC. Finally, linkage disequilibrium (LD) pruning ($r^2 > 0.9$) was applied to yield 977,242 SNPs for which population structure was corrected using PCA (Price et al., 2006).

2.8. Definition of genome nodes

In this study, we used schizophrenia-related SNPs as genetic nodes. Firstly, the SNP with the lowest p value in each of the 108 schizophrenia-associated genetic loci reported by the largest psychiatric genomic consortium (PGC) study (Schizophrenia Working Group of the Psychiatric Genomics, 2014) was identified. SNPs with 0 risk alleles occurring in less than 17 subjects were excluded. This resulted in a set of 81 SNPs selected as gene nodes in the genome-connectome bipartite graph.

2.9. Building the genome-connectome bipartite graph

To build edges in the bipartite graph, we used a general linear model (a MANCOVA framework: http://mialab.mrn.org/software/mancovan) to evaluate the association between each pair of genome-connectome nodes. In this model, for each pair of SNP-FNC, correlation values of all subjects for the FNC connection were input as the dependent variable, and the SNP data coded based on number of risk allele (0, 1, or 2) of all subjects were input as the independent variable. To control sites, groups, and ethnicity effects, they were input as covariates. A significant ($p < 0.05$, uncorrected) association was used to determine whether there is an edge between those two nodes. Finally the degree of each SNP node in the bipartite graph was computed.

2.10. Biclustering analysis

Biclustering is a data mining technique which allows simultaneous clustering of the rows and columns of a matrix (Govaert and Nadif, 2008; Van Mechelen et al., 2004). As a result, submatrices exhibiting unique patterns can be revealed helping us to better understand the relationship between row and column variables (Gupta et al., 2013). To investigate if any subset of SNPs are densely associated with any subset of FNC connections, we performed a biclustering analysis on the SNP-FNC bipartite graph using MTBA (a Matlab toolbox for biclustering analysis) (Gupta et al., 2013).

3. Results:

3.1. Functional brain connectivity

Figure 1A displays the spatial maps of the 50 ICNs identified using group ICA on the fMRI data. Based on their anatomical and presumed functional properties, 50 ICN are arranged into groups of subcortical (SC), auditory (AUD), somato-motor (SM), visual (VIS), cognitive control (CC), default mode (DM), and cerebellum (CB) components. Figure 1B displays the structure of group mean FNC in HCs and SZs. Patterns of FNC are consistent with prior literature, showing modular organization within sensory-cognitive systems and

default mode networks, as well as anti-correlation between these domains (Allen et al., 2014; Fox et al., 2005; Yu et al., 2015; Yu et al., 2011a). In addition, SZs show lower brain connectivity, in line with previous work (Liu et al., 2008; Lynall et al., 2010; Yu et al., 2015; Yu et al., 2011a; Yu et al., 2013b). Figure 1C shows the 83 FNC connections that are selected as fMRI nodes to build the gene-fMRI bipartite graph.

3.2. SNP nodes

Eighty-one schizophrenia-related SNPs were selected as genetic nodes in the genetic-fMRI multimodal bipartite graph. Chromosome 2 had the maximum (10) such number across all 22 chromosomes. For the p values of schizophrenia association of the 81 SNPs and the distribution of them across chromosomes see Figure 2. SNP names are listed in Table 1.

3.3. Bipartite graph

Edges in the bipartite graph between SNP nodes and FNC nodes were determined based on the associations yielded by the general linear model. There are 401 total edges. SNP rs10503253 has the maximum degree of 31 across all 81 SNP nodes. Ten SNPs have a degree value above 10. For the degree of each SNP node see Table 1. Figure 3 shows the structure of this genome-connectome multimodal bipartite graph.

3.4. Biclustering

A biclustering analysis revealed one cluster with 15 SNP nodes and 38 FNC nodes (Figure 4). Most (27) of those 38 FNC nodes are connectivity within or between somato-motor and visual brain components. For spatial brain maps of the 38 FNC pairs see supplemental Figures.

4. Discussion:

In this genome-connectome multimodal study, we proposed a SNP-FNC bipartite graph model. First, fMRI data of HC and SZ were decomposed into 100 spatial components. Then FNC was estimated using 50 components selected as ICNs. Eighty-three FNC connections showing group differences (HCs vs SZs) were chosen as fMRI nodes in the bipartite graph. Eighty-one SNPs previously associated with schizophrenia based on psychiatric genomics consortium (PGC) studies were chosen as genetic nodes. Edges between SNP and FNC were defined by computing the association between SNP node (numbers of risk alleles) and FNC node (correlation values) across subjects using a general linear model. N=401 edges were built in the bipartite graph. Ten SNP nodes are with a degree higher than 10 (see Table 1). A bi-clustering analysis revealed that 15 SNP nodes and 38 FNC nodes are densely associated as a cluster. Most (27) of the 38 FNC nodes are brain connectivity within or between somato-motor and visual components.

To our knowledge, this is the first study which used SNPs and FNC connections as genetic and fMRI nodes respectively to build a genome-connectome multimodal bipartite graph. This model may be widely adopted in a variety of imaging genetic studies. One advantage of the bipartite graph model is that associations between a group of SNPs and a group of connections of brain connectivity may be evaluated in one analysis, rather than most

previous studies that focus only on one or a few candidate SNPs and brain connectivity (Arslan, 2018; Petrella et al., 2008). In addition, both SNP and FNC nodes are schizophrenia-related, and the associations are evaluated across both HCs and SZs, thus the edges in the bipartite graph indicate a consistent relationship in controls and patients.

After computing the degree of each SNP node in the bipartite graph, a total of 10 SNPs (rs10503253, rs4674917, rs7201930, rs79235996, rs604362, rs3784399, rs12623667, rs7267348, rs4908939, rs11693094) had a degree higher than 10 which suggests that they are modulating more functional brain connectivity and may be more strongly associated with the risk of schizophrenia than other SNPs (see Table 1). Future studies may use other methods to validate the possibility of these 10 SNPs carrying more risk for disrupted functional brain connectivity in schizophrenia. A bi-clustering analysis revealed a cluster consisting of 15 SNPs (rs604362, rs9876421, rs11693094, rs7240986, rs67733815, rs1009080, rs3784399, rs4908939, rs79235996, rs10503253, rs4674917, rs7201930, rs12623667, rs12132780, rs7267348) and 38 FNC connections, most (27) of which are within or between somato-motor and visual brain components. These results provide evidence about the genetic basis of disrupted functional brain connectivity in schizophrenia.

However, the findings of this study should be interpreted in light of several methodological limitations. Functional brain connectivity was computed using FNC method in which the brain was firstly decomposed into spatial components. Though a previous simulation study exhibited the benefits of estimating the functional brain network using data driven ICA rather than a fixed atlas based ROI method (Yu et al., 2017), future work may use different approaches (Chong et al., 2017; Cohen et al., 2008; Craddock et al., 2012; Eickhoff et al., 2015; Power et al., 2011; Shen et al., 2010; Wang et al., 2015; Wig et al., 2014; Yeo et al., 2011) to perform brain parcellation for defining brain nodes to compute the functional connectivity. To reduce the number of multiple comparisons when building the edges using general linear model in the gene-fMRI bipartite graph, we just selected a small number of SNPs (81) and FNC connections (83) as nodes. Nevertheless, the edges were still defined via an uncorrected p values ($p < 0.05$). Future studies may include more SNPs and FNC connections, and many more samples (typically thousands of subjects in GWAS studies) to enhance the power of the statistical analysis. To evaluate the statistical probability of the bipartite graph relative to a random one, we built 50000 random bipartite graphs using the same 81 SNP nodes and 83 FNC nodes by randomly re-order the subjects. Results show that the mean degree of each node is 4, and the degree of 11 for any SNP node occurs at about the 10^{th} percentile of the 50000 permutated bipartite graphs.

Conclusions:

This work proposed a new framework for performing image genetics analysis by combining group ICA, bipartite graph analysis, and bi-clustering analysis. We built a genetic-fMRI bipartite graph in which genetic nodes were 81 schizophrenia-related SNPs and fMRI nodes were 83 schizophrenia-related connections of functional brain connectivity. Edges between SNP-FNC nodes which indicate the association between them were assessed using a general linear model across both HCs and SZs. Results showed that 10 SNPs had a degree higher than 10 implying that they modulate functional brain connectivity and may be the most

strongly associated with the risk for schizophrenia. A bi-clustering analysis revealed a cluster with 15 SNPs and 38 connections of the FNC most of which were within or between somato-motor and visual brain components suggesting that brain connectivity in these sensory systems is modulated by a group of SNPs which provides insight for the pathology of schizophrenia. The results of this pilot study suggest that the SNP-FNC bipartite graph may potentially be a powerful model to access the genetic basis of functional brain connectivity as well as that of mental illnesses.

Supplementary Material

Refer to Web version on PubMed Central for supplementary material.

Acknowledgements:

This work is supported by the National Institutes of Health (NIH) grants including a COBRE grant (P20GM103472/5P20RR021938), R01 grants (R01EB005846, 1R01EB006841, 1R01DA040487, R01REB020407, R01EB000840, and R37MH43775) and the National Science Foundation (NSF) grants #1539067, #1618551 and #1631838. This work is also partly supported by the Strategic Priority Research Program of the Chinese Academy of Sciences (XDBS03040100), Brain Initiative of Beijing City (Z181100001518005) Chinese NSF (81471367, 61773380, PI: Sui J; 61703253, PI: YHD) and Natural Science Foundation of Shanxi (2016021077, PI: YHD).”

References:

Adhikari BM, Jahanshad N, Shukla D, Glahn DC, Blangero J, Reynolds RC, Cox RW, Fieremans E, Veraart J, Novikov DS, Nichols TE, Hong LE, Thompson PM, Kochumov PV, 2018 Heritability estimates on resting state fMRI data using ENIGMA analysis pipeline. Pacific Symposium on Biocomputing, Pacific Symposium on Biocomputing 23, 12.

Allen EA, Damaraju E, Plis SM, Erhardt EB, Eichele T, Calhoun VD, 2014 Tracking whole-brain connectivity dynamics in the resting state. Cereb Cortex 24, 663–676. [PubMed: 23146964]

Allen EA, Erhardt EB, Damaraju E, Gruner W, Segall JM, Silva RF, Havlicek M, Rachakonda S, Fries J, Kalyanam R, Michael AM, Caprihan A, Turner JA, Eichele T, Adelsheim S, Bryan AD, Bustillo J, Clark VP, Feldstein Ewing SW, Filbey F, Ford CC, Hutchison K, Jung RE, Kiehl KA, Kodituwakku P, Komesu YM, Mayer AR, Pearlson GD, Phillips JP, Sadek JR, Stevens M, Teuscher U, Thoma RJ, Calhoun VD, 2011 A baseline for the multivariate comparison of resting-state networks. Front Syst Neurosci 5, 2. [PubMed: 21442040]

Altshuler DM, Durbin RM, Abecasis GR, Bentley DR, Chakravarti A, Clark AG, Donnelly P, Eichler EE, Flicek P, Gabriel SB, Gibbs RA, Green ED, Hurles ME, Knoppers BM, Korbel JO, Lander ES, Lee C, Lehrach H, Mardis ER, Marth GT, McVean GA, Nickerson DA, Schmidt JP, Sherry ST, Wang J, Wilson RK, Gibbs RA, Dinh H, Kovar C, Lee S, Lewis L, Muzny D, Reid J, Wang M, Wang J, Fang XD, Guo XS, Jian M, Jiang H, Jin X, Li GQ, Li JX, Li YR, Li Z, Liu X, Lu Y, Ma XD, Su Z, Tai SS, Tang MF, Wang B, Wang GB, Wu HL, Wu RH, Yin Y, Zhang WW, Zhao J, Zhao MR, Zheng XL, Zhou Y, Lander ES, Altshuler DM, Gabriel SB, Gupta N, Flicek P, Clarke L, Leinonen R, Smith RE, Zheng-Bradley X, Bentley DR, Grocock R, Humphray S, James T, Kingsbury Z, Lehrach H, Sudbrak R, Albrecht MW, Amstislavskiy VS, Borodina TA, Lienhard M, Mertes F, Sultan M, Timmermann B, Yaspo ML, Sherry ST, McVean GA, Mardis ER, Wilson RK, Fulton L, Fulton R, Weinstock GM, Durbin RM, Balasubramaniam S, Burton J, Danecek P, Keane TM, Kolb-Kokocinski A, McCarthy S, Stalker J, Quail M, Schmidt JP, Davies CJ, Gollub J, Webster T, Wong B, Zhan YP, Auton A, Gibbs RA, Yu F, Bainbridge M, Challis D, Evani US, Lu J, Muzny D, Nagaswamy U, Reid J, Sabo A, Wang Y, Yu J, Wang J, Coin LJM, Fang L, Guo XS, Jin X, Li GQ, Li QB, Li YR, Li ZY, Lin HX, Liu BH, Luo RB, Qin N, Shao HJ, Wang BQ, Xie YL, Ye C, Yu C, Zhang F, Zheng HC, Zhu HM, Marth GT, Garrison EP, Kural D, Lee WP, Leong WF, Ward AN, Wu JT, Zhang MY, Lee C, Griffin L, Hsieh CH, Mills RE, Shi XH, von Grotthuss M, Zhang CS, Daly MJ, DePristo MA, Altshuler DM, Banks E, Bhatia G, Carneiro MO, del Angel G, Gabriel SB, Genovese G, Gupta N, Handsaker RE, Hartl C, Lander ES, McCarroll SA, Nemesh JC, Poplin RE,

Schaffner SF, Shakir K, Yoon SC, Lihm J, Makarov V, Jin HJ, Kim W, Kim KC, Korbel JO, Rausch T, Flicek P, Beal K, Clarke L, Cunningham F, Herrero J, McLaren WM, Ritchie GRS, Smith RE, Zheng-Bradley X, Clark AG, Gottipati S, Keinan A, Rodriguez-Flores JL, Sabeti PC, Grossman SR, Tabrizi S, Tariyal R, Cooper DN, Ball EV, Stenson PD, Bentley DR, Barnes B, Bauer M, Cheetham RK, Cox T, Eberle M, Humphray S, Kahn S, Murray L, Peden J, Shaw R, Ye K, Batzer MA, Konkel MK, Walker JA, MacArthur DG, Lek M, Sudbrak R, Amstislavskiy VS, Herwig R, Shriver MD, Bustamante CD, Byrnes JK, De la Vega FM, Gravel S, Kenny EE, Kidd JM, Lacroute P, Maples BK, Moreno-Estrada A, Zakharia F, Halperin E, Baran Y, Craig DW, Christoforides A, Homer N, Izatt T, Kurdoglu AA, Sinari SA, Squire K, Sherry ST, Xiao CL, Sebat J, Bafna V, Ye K, Burchard EG, Hernandez RD, Gignoux CR, Haussler D, Katzman SJ, Kent WJ, Howie B, Ruiz-Linares A, Dermitzakis ET, Lappalainen T, Devine SE, Liu XY, Maroo A, Tallon LJ, Rosenfeld JA, Michelson LP, Abecasis GR, Kang HM, Anderson P, Angius A, Bigham A, Blackwell T, Busonero F, Cucca F, Fuchsberger C, Jones C, Jun G, Li Y, Lyons R, Maschio A, Porcu E, Reinier F, Sanna S, Schlessinger D, Sidore C, Tan A, Trost MK, Awadalla P, Hodgkinson A, Lunter G, McVean GA, Marchini JL, Myers S, Churchhouse C, Delaneau O, Gupta-Hinch A, Iqbal Z, Mathieson I, Rimmer A, Xifara DK, Oleksyk TK, Fu YX, Liu XM, Xiong MM, Jorde L, Witherspoon D, Xing JC, Eichler EE, Browning BL, Alkan C, Hajirasouliha I, Hormozdiari F, Ko A, Sudmant PH, Mardis ER, Chen K, Chinwalla A, Ding L, Dooling D, Koboldt DC, McLellan MD, Wallis JW, Wendl MC, Zhang QY, Durbin RM, Hurles ME, Tyler-Smith C, Albers CA, Ayub Q, Balasubramaniam S, Chen Y, Coffey AJ, Colonna V, Danecek P, Huang N, Jostins L, Keane TM, Li H, McCarthy S, Scally A, Stalker J, Walter K, Xue YL, Zhang YJ, Gerstein MB, Abyzov A, Balasubramanian S, Chen JM, Clarke D, Fu Y, Habegger L, Harmanci AO, Jin MK, Khurana E, Mu XJ, Sisu C, Li YR, Luo RB, Zhu HM, Lee C, Griffin L, Hsieh CH, Mills RE, Shi XH, von Grotthuss M, Zhang CS, Marth GT, Garrison EP, Kural D, Lee WP, Ward AN, Wu JT, Zhang MY, McCarroll SA, Altshuler DM, Banks E, del Angel G, Genovese G, Handsaker RE, Hartl C, Nemesh JC, Shakir K, Yoon SC, Lihm J, Makarov V, Degenhardt J, Flicek P, Clarke L, Smith RE, Zheng-Bradley X, Korbel JO, Rausch T, Stutz AM, Bentley DR, Barnes B, Cheetham RK, Eberle M, Humphray S, Kahn S, Murray L, Shaw R, Ye K, Batzer MA, Konkel MK, Walker JA, Lacroute P, Craig DW, Homer N, Church D, Xiao CL, Sebat J, Bafna V, Michaelson JJ, Ye K, Devine SE, Liu XY, Maroo A, Tallon LJ, Lunter G, McVean GA, Iqbal Z, Witherspoon D, Xing JC, Eichler EE, Alkan C, Hajirasouliha I, Hormozdiari F, Ko A, Sudmant PH, Chen K, Chinwalla A, Ding L, McLellan MD, Wallis JW, Hurles ME, Blackburne B, Li H, Lindsay SJ, Ning ZM, Scally A, Walter K, Zhang YJ, Gerstein MB, Abyzov A, Chen JM, Clarke D, Khurana E, Mu XJ, Sisu C, Gibbs RA, Yu FL, Bainbridge M, Challis D, Evani US, Kovar C, Lewis L, Lu J, Muzny D, Nagaswamy U, Reid J, Sabo A, Yu J, Guo XS, Li YR, Wu RH, Marth GT, Garrison EP, Leong WF, Ward AN, del Angel G, DePristo MA, Gabriel SB, Gupta N, Hartl C, Poplin RE, Clark AG, Rodriguez-Flores JL, Flicek P, Clarke L, Smith RE, Zheng-Bradley X, MacArthur DG, Bustamante CD, Gravel S, Craig DW, Christoforides A, Homer N, Izatt T, Sherry ST, Xiao CL, Dermitzakis ET, Abecasis GR, Kang HM, McVean GA, Mardis ER, Dooling D, Fulton L, Fulton R, Koboldt DC, Durbin RM, Balasubramaniam S, Keane TM, McCarthy S, Stalker J, Gerstein MB, Balasubramanian S, Habegger L, Garrison EP, Gibbs RA, Bainbridge M, Muzny D, Yu FL, Yu J, del Angel G, Handsaker RE, Makarov V, Rodriguez-Flores JL, Jin HJ, Kim W, Kim KC, Flicek P, Beal K, Clarke L, Cunningham F, Herrero J, McLaren WM, Ritchie GRS, Zheng-Bradley X, Tabrizi S, MacArthur DG, Lek M, Bustamante CD, De la Vega FM, Craig DW, Kurdoglu AA, Lappalainen T, Rosenfeld JA, Michelson LP, Awadalla P, Hodgkinson A, McVean GA, Chen K, Tyler-Smith C, Chen Y, Colonna V, Frankish A, Harrow J, Xue YL, Gerstein MB, Abyzov A, Balasubramanian S, Chen JM, Clarke D, Fu Y, Harmanci AO, Jin MK, Khurana E, Mu XJ, Sisu C, Gibbs RA, Fowler G, Hale W, Kalra D, Kovar C, Muzny D, Reid J, Wang J, Guo X, Li G, Li Y, Zheng X, Altshuler DM, Flicek P, Clarke L, Barker J, Kelman G, Kulesha E, Leinonen R, McLaren WM, Radhakrishnan R, Roa A, Smirnov D, Smith RE, Streeter I, Toneva I, Vaughan B, Zheng-Bradley X, Bentley DR, Cox T, Humphray S, Kahn S, Sudbrak R, Albrecht MW, Lienhard M, Craig DW, Izatt T, Kurdoglu AA, Sherry ST, Ananiev V, Belaia Z, Beloslyudtsev D, Bouk N, Chen C, Church D, Cohen R, Cook C, Garner J, Hefferon T, Kimelman M, Liu C, Lopez J, Meric P, O'Sullivan C, Ostapchuk Y, Phan L, Ponomarov S, Schneider V, Shekhtman E, Sirotkin K, Slotta D, Xiao CL, Zhang H, Haussler D, Abecasis GR, McVean GA, Alkan C, Ko A, Dooling D, Durbin RM, Balasubramaniam S, Keane TM, McCarthy S, Stalker J, Chakravarti A, Knoppers BM, Abecasis GR, Barnes KC, Beiswanger C, Burchard EG, Bustamante CD, Cai HY, Cao HZ, Durbin RM, Gharani N, Gibbs RA, Gignoux CR, Gravel S, Henn B, Jones D, Jorde L, Kaye JS, Keinan A,

Kent A, Kerasidou A, Li YR, Mathias R, McVean GA, Moreno-Estrada A, Ossorio PN, Parker M, Reich D, Rotimi CN, Royal CD, Sandoval K, Su YY, Sudbrak R, Tian ZM, Timmermann B, Tishkoff S, Toji LH, Tyler-Smith C, Via M, Wang YH, Yang HM, Yang L, Zhu JY, Bodmer W, Bedoya G, Ruiz-Linares A, Ming CZ, Yang G, You CJ, Peltonen L, Garcia-Montero A, Orfao A, Dutil J, Martinez-Cruzado JC, Oleksyk TK, Brooks LD, Felsenfeld AL, McEwen JE, Clemm NC, Duncanson A, Dunn M, Green ED, Guyer MS, Peterson JL, Abecasis GR, Auton A, Brooks LD, DePristo MA, Durbin RM, Handsaker RE, Kang HM, Marth GT, McVean GA, Consortium GP, 2012 An integrated map of genetic variation from 1,092 human genomes. Nature 491, 56–65. [PubMed: 23128226]

Anokhin AP, 2014 Genetic psychophysiology: advances, problems, and future directions. Int J Psychophysiol 93, 173–197. [PubMed: 24739435]

Arbabshirani MR, Calhoun VD, 2011 Functional network connectivity during rest and task: comparison of healthy controls and schizophrenic patients. Conf Proc IEEE Eng Med Biol Soc 2011, 4418–4421. [PubMed: 22255319]

Arbabshirani MR, Kiehl KA, Pearlson GD, Calhoun VD, 2013 Classification of schizophrenia patients based on resting-state functional network connectivity. Front Neurosci 7, 133. [PubMed: 23966903]

Arbabshirani MR, Plis S, Sui J, Calhoun VD, 2017 Single subject prediction of brain disorders in neuroimaging: Promises and pitfalls. Neuroimage 145, 137–165. [PubMed: 27012503]

Arslan A, 2018 Mapping the Schizophrenia Genes by Neuroimaging: The Opportunities and the Challenges. Int J Mol Sci 19.

Bell AJ, Sejnowski TJ, 1995 An information-maximization approach to blind separation and blind deconvolution. Neural Comput 7, 1129–1159. [PubMed: 7584893]

Betzel RF, Bassett DS, 2016 Multi-scale brain networks. Neuroimage.

Biswal B, Yetkin FZ, Haughton VM, Hyde JS, 1995 Functional connectivity in the motor cortex of resting human brain using echo-planar MRI. Magn Reson Med 34, 537–541. [PubMed: 8524021]

Biswal BB, 2012 Resting state fMRI: a personal history. Neuroimage 62, 938–944. [PubMed: 22326802]

Brualdi RA, Harary F, Miller Z, 1980 Bigraphs Versus Digraphs Via Matrices. Journal of Graph Theory 4, 51–73.

Calhoun VD, Adali T, Pearlson GD, Pekar JJ, 2001 A method for making group inferences from functional MRI data using independent component analysis. Hum Brain Mapp 14, 140–151. [PubMed: 11559959]

Chen J, Calhoun VD, Lin D, Perrone-Bizzozero NI, Bustillo JR, Pearlson GD, Potkin SG, Van Erp TG, Macciardi F, Ehrlich S, 2018 Shared Genetic Risk of Schizophrenia and Gray Matter Reduction in 6p22. 1. Schizophrenia Bulletin Epub.

Chen J, Calhoun VD, Pearlson GD, Perrone-Bizzozero N, Sui J, Turner JA, Bustillo JR, Ehrlich S, Sponheim SR, Canive JM, Ho BC, Liu J, 2013 Guided exploration of genomic risk for gray matter abnormalities in schizophrenia using parallel independent component analysis with reference. Neuroimage 83C, 384–396.

Chong M, Bhushan C, Joshi AA, Choi S, Haldar JP, Shattuck DW, Spreng RN, Leahy RM, 2017 Individual parcellation of resting fMRI with a group functional connectivity prior. Neuroimage 156, 87–100. [PubMed: 28478226]

Cohen AL, Fair DA, Dosenbach NUF, Miezin FM, Dierker D, Van Essen DC, Schlaggar BL, Petersen SE, 2008 Defining functional areas in individual human brains using resting functional connectivity MRI. Neuroimage 41, 45–57. [PubMed: 18367410]

Craddock RC, James GA, Holtzheimer PE 3rd, Hu XP, Mayberg HS, 2012 A whole brain fMRI atlas generated via spatially constrained spectral clustering. Hum Brain Mapp 33, 1914–1928. [PubMed: 21769991]

Damaraju E, Allen EA, Belger A, Ford JM, McEwen S, Mathalon DH, Mueller BA, Pearlson GD, Potkin SG, Preda A, Turner JA, Vaidya JG, van Erp TG, Calhoun VD, 2014 Dynamic functional connectivity analysis reveals transient states of dysconnectivity in schizophrenia. Neuroimage Clin 5, 298–308. [PubMed: 25161896]

Delaneau O, Marchini J, Zagury JF, 2011 A linear complexity phasing method for thousands of genomes. Nat Methods 9, 179–181. [PubMed: 22138821]

Du YH, L FS, Lin DD, Sui J, Yu QB, Chen JY, Stuart B, Loewy, Calhoun VD, Mathalon, 2018 Identifying functional network changing patterns in individuals at clinical high-risk for psychosis and patients with early illness schizophrenia: A group ICA study. Neuroimage Clin 17, 335–346. [PubMed: 29159045]

Du YH, Pearlson GD, Liu JY, Sui J, Yu QB, He H, Castro E, Calhoun VD, 2015 A group ICA based framework for evaluating resting fMRI markers when disease categories are unclear: application to schizophrenia, bipolar, and schizoaffective disorders. Neuroimage 122, 272–280. [PubMed: 26216278]

Eickhoff SB, Thirion B, Varoquaux G, Bzdok D, 2015 Connectivity-based parcellation: Critique and implications. Hum Brain Mapp 36, 4771–4792. [PubMed: 26409749]

Erhardt EB, Rachakonda S, Bedrick EJ, Allen EA, Adali T, Calhoun VD, 2011 Comparison of multi-subject ICA methods for analysis of fMRI data. Hum Brain Mapp 32, 2075–2095. [PubMed: 21162045]

Fox MD, Raichle ME, 2007 Spontaneous fluctuations in brain activity observed with functional magnetic resonance imaging. Nat Rev Neurosci 8, 700–711. [PubMed: 17704812]

Fox MD, Snyder AZ, Vincent JL, Corbetta M, Van Essen DC, Raichle ME, 2005 The human brain is intrinsically organized into dynamic, anticorrelated functional networks. Proc Natl Acad Sci U S A 102, 9673–9678. [PubMed: 15976020]

Freire L, Roche A, Mangin JF, 2002 What is the best similarity measure for motion correction in fMRI time series? IEEE Trans Med Imaging 21, 470–484. [PubMed: 12071618]

Friedman L, Glover GH, Fbirn C, 2006a Reducing interscanner variability of activation in a multicenter fMRI study: controlling for signal-to-fluctuation-noise-ratio (SFNR) differences. Neuroimage 33, 471–481. [PubMed: 16952468]

Friedman L, Glover GH, Krenz D, Magnotta V, First B, 2006b Reducing inter-scanner variability of activation in a multicenter fMRI study: role of smoothness equalization. Neuroimage 32, 1656–1668. [PubMed: 16875843]

Friston KJ, 2011 Functional and effective connectivity: a review. Brain Connect 1, 13–36. [PubMed: 22432952]

Friston KJ, Frith CD, Fletcher P, Liddle PF, Frackowiak RS, 1996 Functional topography: multidimensional scaling and functional connectivity in the brain. Cereb Cortex 6, 156–164. [PubMed: 8670646]

Fu Y, Ma Z, Hamilton C, Liang Z, Hou X, Ma X, Hu X, He Q, Deng W, Wang Y, Zhao L, Meng H, Li T, Zhang N, 2015 Genetic influences on resting-state functional networks: A twin study. Hum Brain Mapp 36, 3959–3972. [PubMed: 26147340]

Ge T, Holmes AJ, Buckner RL, Smoller JW, Sabuncu MR, 2017 Heritability analysis with repeat measurements and its application to resting-state functional connectivity. Proc Natl Acad Sci U S A 114, 5521–5526. [PubMed: 28484032]

Glahn DC, Winkler AM, Kochunov P, Almasy L, Duggirala R, Carless MA, Curran JC, Olvera RL, Laird AR, Smith SM, Beckmann CF, Fox PT, Blangero J, 2010 Genetic control over the resting brain. Proc Natl Acad Sci U S A 107, 1223–1228. [PubMed: 20133824]

Govaert G, Nadif M, 2008 Block clustering with Bernoulli mixture models: Comparison of different approaches. Computational Statistics & Data Analysis 52, 3233–3245.

Gupta JK, Singh S, Verma NK, 2013 MTBA: matlab toolbox for biclustering analysis. IEEE workshop on computational intelligence: theories, applications and future directions, IIT Kanpur, India., 4.

He H, Yu Q, Du Y, Vergara V, Victor TA, Drevets WC, Savitz JB, Jiang T, Sui J, Calhoun VD, 2016 Resting-state functional network connectivity in prefrontal regions differs between unmedicated patients with bipolar and major depressive disorders. J Affect Disord 190, 483–493. [PubMed: 26551408]

Jafri MJ, Pearlson GD, Stevens M, Calhoun VD, 2008 A method for functional network connectivity among spatially independent resting-state components in schizophrenia. Neuroimage 39, 1666–1681. [PubMed: 18082428]

Liu Y, Liang M, Zhou Y, He Y, Hao Y, Song M, Yu C, Liu H, Liu Z, Jiang T, 2008 Disrupted small-world networks in schizophrenia. Brain 131, 945–961. [PubMed: 18299296]

Lynall ME, Bassett DS, Kerwin R, McKenna PJ, Kitzbichler M, Muller U, Bullmore E, 2010 Functional connectivity and brain networks in schizophrenia. J Neurosci 30, 9477–9487. [PubMed: 20631176]

Ma S, Correa NM, Li XL, Eichele T, Calhoun VD, Adali T, 2011 Automatic Identification of Functional Clusters in fMRI Data Using Spatial Dependence. Ieee Transactions on Biomedical Engineering 58, 3406–3417. [PubMed: 21900068]

Marchini J, Howie B, 2010 Genotype imputation for genome-wide association studies. Nat Rev Genet 11, 499–511. [PubMed: 20517342]

Meyer-Lindenberg A, Weinberger DR, 2006 Intermediate phenotypes and genetic mechanisms of psychiatric disorders. Nature Reviews Neuroscience 7, 818–827. [PubMed: 16988657]

Petrella JR, Mattay VS, Doraiswamy PM, 2008 Imaging genetics of brain longevity and mental wellness: the next frontier? Radiology 246, 20–32. [PubMed: 18096526]

Potkin SG, Turner JA, Guffanti G, Lakatos A, Fallon JH, Nguyen DD, Mathalon D, Ford J, Lauriello J, Macciardi F, Fbirn, 2009 A genome-wide association study of schizophrenia using brain activation as a quantitative phenotype. Schizophr Bull 35, 96–108. [PubMed: 19023125]

Power JD, Cohen AL, Nelson SM, Wig GS, Barnes KA, Church JA, Vogel AC, Laumann TO, Miezin FM, Schlaggar BL, Petersen SE, 2011 Functional Network Organization of the Human Brain. Neuron 72, 665–678. [PubMed: 22099467]

Price AL, Patterson NJ, Plenge RM, Weinblatt ME, Shadick NA, Reich D, 2006 Principal components analysis corrects for stratification in genome-wide association studies. Nature Genetics 38, 904–909. [PubMed: 16862161]

Purcell S, Neale B, Todd-Brown K, Thomas L, Ferreira MA, Bender D, Maller J, Sklar P, de Bakker PI, Daly MJ, Sham PC, 2007 PLINK: a tool set for whole-genome association and population-based linkage analyses. American Journal of Human Genetics 81, 559–575. [PubMed: 17701901]

Schizophrenia Working Group of the Psychiatric Genomics, C., 2014 Biological insights from 108 schizophrenia-associated genetic loci. Nature 511, 421–427. [PubMed: 25056061]

Shen X, Papademetris X, Constable RT, 2010 Graph-theory based parcellation of functional subunits in the brain from resting-state fMRI data. Neuroimage 50, 1027–1035. [PubMed: 20060479]

Sinclair B, Hansell NK, Blokland GA, Martin NG, Thompson PM, Breakspear M, de Zubicaray GI, Wright MJ, McMahon KL, 2015 Heritability of the network architecture of intrinsic brain functional connectivity. Neuroimage 121, 243–252. [PubMed: 26226088]

Sullivan PF, Kendler KS, Neale MC, 2003 Schizophrenia as a complex trait - Evidence from a meta-analysis of twin studies. Archives of General Psychiatry 60, 1187–1192. [PubMed: 14662550]

van den Heuvel MP, Fornito A, 2014 Brain networks in schizophrenia. Neuropsychol Rev 24, 32–48. [PubMed: 24500505]

van den Heuvel MP, Hulshoff Pol HE, 2010 Exploring the brain network: a review on resting-state fMRI functional connectivity. Eur Neuropsychopharmacol 20, 519–534. [PubMed: 20471808]

van den Heuvel MP, van Soelen ILC, Stam CJ, Kahn RS, Boomsma DI, Pol HEH, 2013 Genetic control of functional brain network efficiency in children. European Neuropsychopharmacology 23, 19–23. [PubMed: 22819192]

Van Mechelen I, Bock HH, De Boeck P, 2004 Two-mode clustering methods: a structured overview. Stat Methods Med Res 13, 363–394. [PubMed: 15516031]

Wang D, Buckner RL, Fox MD, Holt DJ, Holmes AJ, Stoecklein S, Langs G, Pan R, Qian T, Li K, Baker JT, Stufflebeam SM, Wang K, Wang X, Hong B, Liu H, 2015 Parcellating cortical functional networks in individuals. Nat Neurosci 18, 1853–1860. [PubMed: 26551545]

Wig GS, Laumann TO, Petersen SE, 2014 An approach for parcellating human cortical areas using resting-state correlations. Neuroimage 93 Pt 2, 276–291.

Xu J, Yin X, Ge H, Han Y, Pang Z, Liu B, Liu S, Friston K, 2017 Heritability of the Effective Connectivity in the Resting-State Default Mode Network. Cereb Cortex 27, 5626–5634. [PubMed: 27913429]

Yang Z, Zuo XN, McMahon KL, Craddock RC, Kelly C, de Zubicaray GI, Hickie I, Bandettini PA, Castellanos FX, Milham MP, Wright MJ, 2016 Genetic and Environmental Contributions to Functional Connectivity Architecture of the Human Brain. Cereb Cortex 26, 2341–2352. [PubMed: 26891986]

Yeo BT, Krienen FM, Sepulcre J, Sabuncu MR, Lashkari D, Hollinshead M, Roffman JL, Smoller JW, Zollei L, Polimeni JR, Fischl B, Liu H, Buckner RL, 2011 The organization of the human cerebral cortex estimated by intrinsic functional connectivity. J Neurophysiol 106, 1125–1165. [PubMed: 21653723]

Yu Q, Du Y, Chen J, He H, Sui J, Pearlson G, Calhoun VD, 2017 Comparing brain graphs in which nodes are regions of interest or independent components: A simulation study. J Neurosci Methods 291, 61–68. [PubMed: 28807861]

Yu Q, Du Y, Chen J, Sui J, Adali T, Pearlson G, Calhoun V, 2018 Application of Graph Theory to Assess Static and Dynamic Brain Connectivity: Approaches for Building Brain Graphs. Proceedings of the IEEE 106, 21.

Yu Q, Erhardt EB, Sui J, Du Y, He H, Hjelm D, Cetin MS, Rachakonda S, Miller RL, Pearlson G, Calhoun VD, 2015 Assessing dynamic brain graphs of time-varying connectivity in fMRI data: application to healthy controls and patients with schizophrenia. Neuroimage 107, 345–355. [PubMed: 25514514]

Yu Q, Plis SM, Erhardt EB, Allen EA, Sui J, Kiehl KA, Pearlson G, Calhoun VD, 2011a Modular Organization of Functional Network Connectivity in Healthy Controls and Patients with Schizophrenia during the Resting State. Frontiers in systems neuroscience 5, 103. [PubMed: 22275887]

Yu Q, Sui J, Kiehl KA, Pearlson G, Calhoun VD, 2013a State-related functional integration and functional segregation brain networks in schizophrenia. Schizophr Res 150, 450–458. [PubMed: 24094882]

Yu Q, Sui J, Liu J, Plis SM, Kiehl KA, Pearlson G, Calhoun VD, 2013b Disrupted correlation between low frequency power and connectivity strength of resting state brain networks in schizophrenia. Schizophrenia research 143, 165–171. [PubMed: 23182443]

Yu Q, Sui J, Rachakonda S, He H, Gruner W, Pearlson G, Kiehl KA, Calhoun VD, 2011b Altered topological properties of functional network connectivity in schizophrenia during resting state: a small-world brain network study. PloS one 6, e25423. [PubMed: 21980454]

Highlights

- A genome-connectome bipartite graph model for imaging genomic analysis.
- We used this model to explore associations of schizophrenia-related genetic variants with group-discriminative functional connectivity features.
- Genetic nodes with high degree in the bipartite graph were identified to indicate their role in modulating brain connectivity.
- A bi-clustering analysis detected a cluster where 15 genetic variants interact with 38 functional connectivity features.

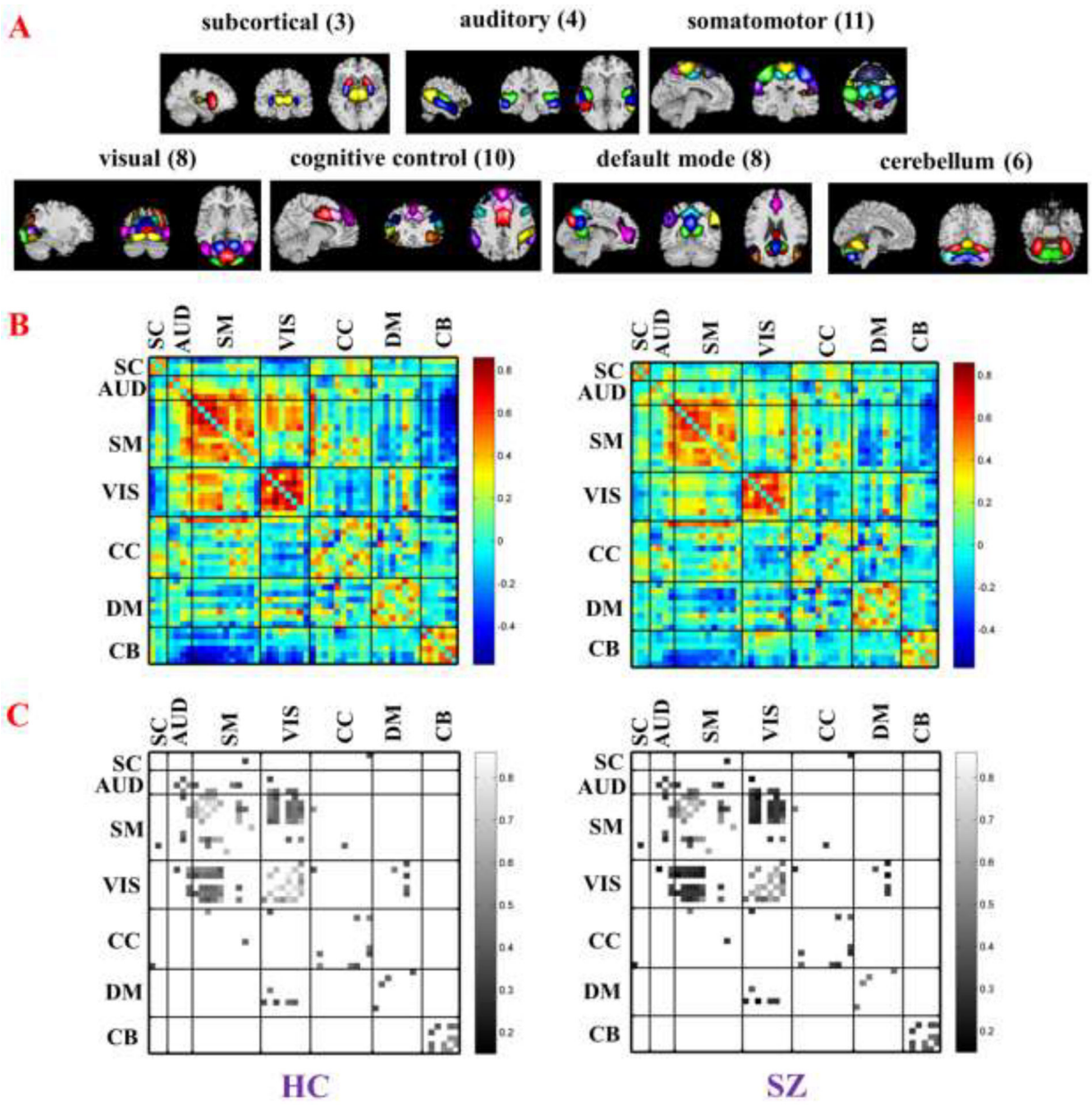

Figure 1.

Spatial maps (A) of 50 brain components selected to compute functional network connectivity (FNC). Brain components are divided into groups and arranged based on their anatomical and functional properties. Structure of group mean FNC (B. HC: healthy controls; SZ: patients with schizophrenia) shows that brain connectivity is lower in SZ. Eighty three connections (C) in the FNC are selected to be fMRI nodes for constructing the gene-fMRI bipartite graph. (SC: subcortical; AUD: auditory; SM: somatomotor; VIS: visual; CC: cognitive control; DM: default mode; CB: cerebellum)

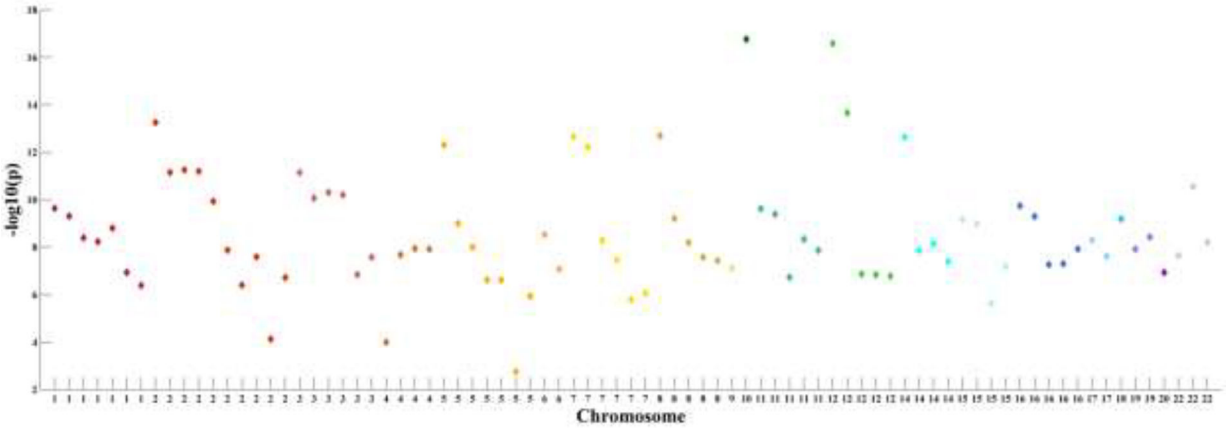

Figure 2.

Scatter plot showing schizophrenia-related associations of the selected SNPs as genetic nodes and their distribution across chromosomes. The x axis is chromosomal position and the y axis is the significance (-log10(p)) of association as reported by the PGC study (Schizophrenia Working Group of the Psychiatric Genomics, 2014).

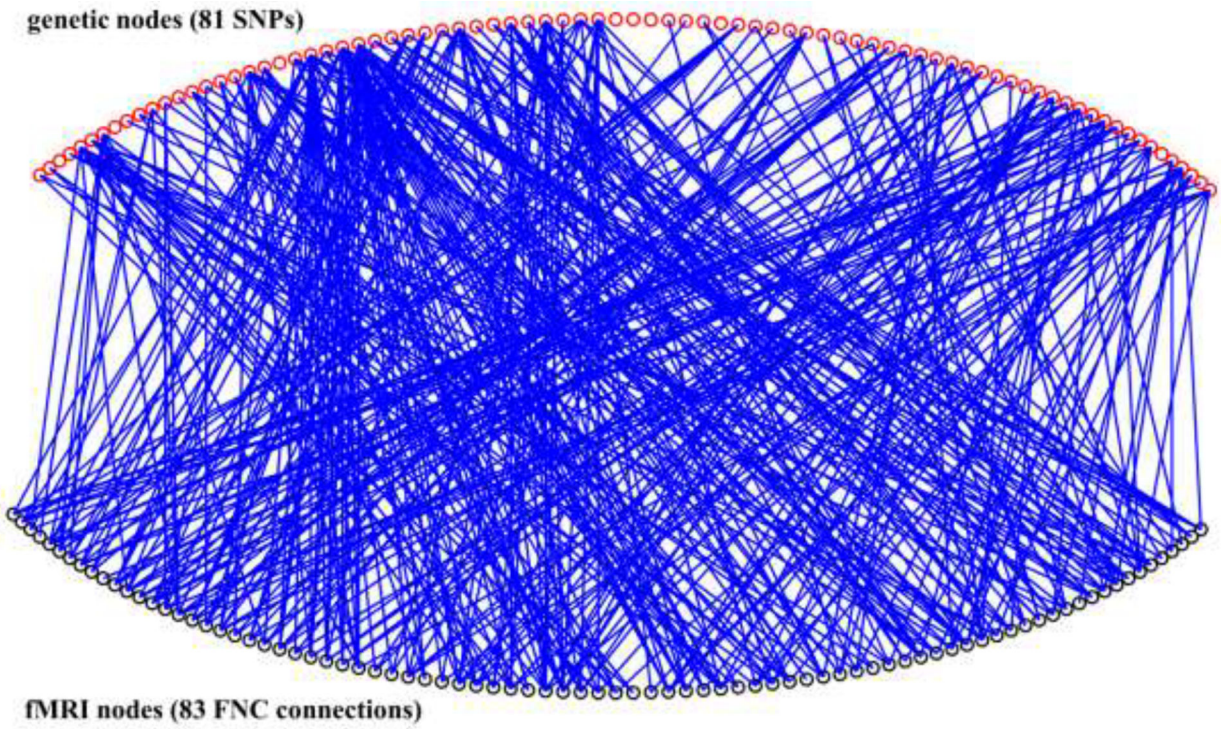

Figure 3.
Structure of the gene-fMRI bipartite graph. Some SNP nodes are showing high degree (> 10, see Table 1).

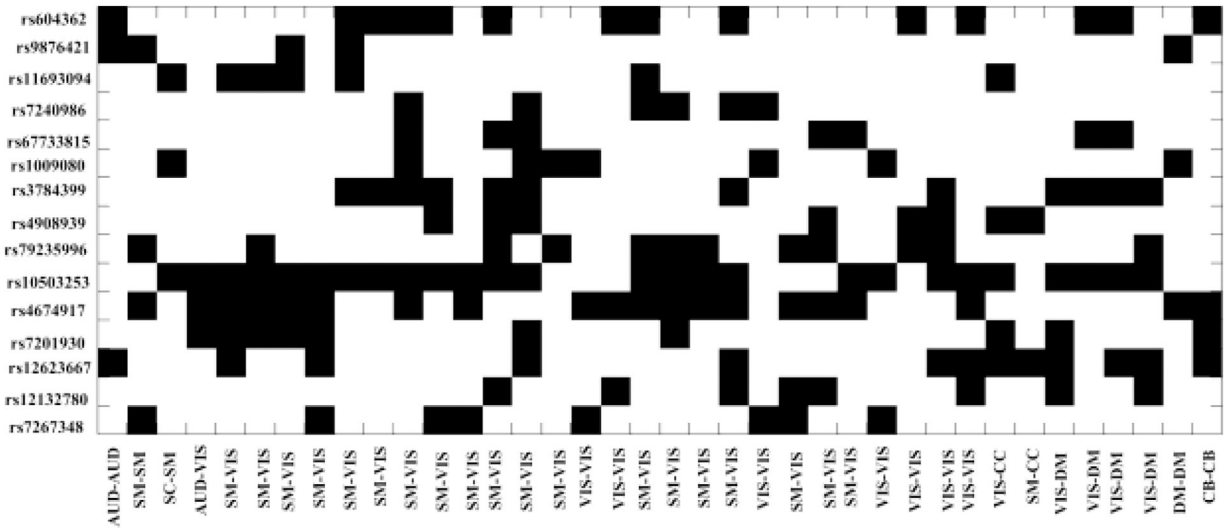

Figure 4.
Cluster with 15 SNP nodes and 38 FNC nodes detected by biclustering analysis.

Table 1.

Eighty-one SNP nodes and their degree in the gene-fMRI bipartite graph (chromosomal positions based on hg19 genome assembly).

SNP rsID	chromosome	position	degree	SNP rsID	chromosome	position	degree	SNP rsID	chromosome	position	degree
rs10503253	8	4180844	31	rs778341	2	233728801	5	rs9906500	17	2129210	2
rs4674917	2	225387522	24	rs2068012	14	30190316	5	rs12903146	15	61854663	2
rs7201930	16	9958655	21	rs12129573	1	73768366	4	rs4648845	1	2387101	2
rs79235996	14	72419030	15	rs9611520	22	41613303	4	rs67401222	1	8490320	2
rs604362	4	103147494	14	rs4481150	3	52837793	4	rs1209749	9	84802861	2
rs3784399	15	40598294	14	rs5995756	22	40000313	4	rs12446487	16	58671815	2
rs12623667	2	149405178	14	rs1501362	5	45378207	4	rs7722581	5	153676440	2
rs7267348	20	48131036	13	rs10206411	2	193933194	4	rs10860955	12	103581985	2
rs4908939	3	17793850	12	rs7197756	16	68275516	4	rs6867549	5	140153730	2
rs11693094	2	185601420	11	rs12939020	17	17950163	4	rs2007044	12	2344960	1
rs1009080	1	30431560	9	rs2789605	6	73155289	4	rs7108770	11	46648432	1
rs34026011	14	104050883	8	rs215411	4	23423603	4	rs2973155	5	152608619	1
rs11210892	1	44100084	8	rs4129585	8	143312933	3	rs34538000	19	19481379	1
rs12132780	1	207999605	8	rs11688767	2	57988194	3	rs217326	6	84349538	1
rs7896519	10	104866863	7	rs16880919	8	111620054	3	rs7438	4	170642246	1
rs7240986	18	53195249	7	rs2053079	19	30987423	3	rs134900	22	42683343	1
rs67733815	3	2549591	7	rs11956240	5	137840293	3	rs2693698	14	99719219	1
rs4788190	16	29948401	7	rs6846161	4	176866459	3	rs17149781	7	24695495	1
rs6670165	1	177280121	7	rs7838490	8	89585048	3	rs211792	7	110072128	1
rs2851447	12	123665113	6	rs1355585	15	70586617	3	rs4546329	5	60589739	0
rs9876421	3	36848316	6	rs2300990	5	109033393	3	rs12705304	7	104929633	0
rs1076884	16	13747803	6	rs10745572	12	92252357	3	rs68002929	2	146419989	0
rs4728408	7	137072096	6	rs8039305	15	91422543	2	rs11229116	11	57534542	0
rs7018304	8	60717504	6	rs13240464	7	110898915	2	rs1470276	11	24397676	0
rs7927176	11	123395864	6	rs787983	2	198345797	2	rs832190	3	63842629	0
rs13227554	7	2048220	5	rs2514218	11	113392994	2	rs302321	12	29928388	0
rs11693528	2	200736507	5	rs66691851	3	136154828	2	rs2909456	2	162836954	0